Sphingosine kinases: emerging structure-function insights

David R. Adams[1], Susan Pyne[2] and Nigel J. Pyne[2*]

[1]Institute of Chemical Sciences, Heriot-Watt University, Edinburgh, EH14 4AS, Scotland, UK; [2]Strathclyde Institute of Pharmacy and Biomedical Sciences, University of Strathclyde, 161 Cathedral St, Glasgow, G4 0RE, Scotland, UK

*Correspondence: n.j.pyne@strath.ac.uk

Keywords

Sphingosine kinase (SK1, SK2), DAGK_cat, diacylglycerol kinase (DGK), membrane curvature, TRAF2

Abstract

Sphingosine kinases (SK1 and SK2) catalyse the conversion of sphingosine into sphingosine 1-phosphate and control fundamental cellular processes, including cell survival, proliferation, differentiation, migration and immune function. In this Review, we highlight recent breakthroughs in the structural and functional characterisation of SK1 and these are contextualized by analysis of crystal structures for closely related prokaryotic lipid kinases. We identify a putative dimerisation interface and propose novel regulatory mechanisms governing structural plasticity induced by phosphorylation and interaction with phospholipids and proteins. Our analysis suggests that the catalytic function and regulation of the enzymes might be dependent on conformational mobility and it provides a roadmap for future interrogation of SK1 function and its role in physiology and disease.

Pivotal signalling roles of sphingosine kinases

Sphingosine 1-phosphate (S1P) is an endogenous pleiotropic lipid mediator that regulates many physiological effects, including modulation of the vascular barrier integrity and tone, angiogenesis and trafficking of immune cells [1]. However, S1P also has a pathophysiological role in autoimmune dysfunction, inflammation, cancer and many other diseases [2-4]. S1P binds to and activates a family of five S1P-specific G protein-coupled receptors, $S1P_1$-$S1P_5$, following its release from cells through transporter proteins [5, 6]. A number of intracellular target proteins of S1P have also been identified, including histone deacetylases (HDAC1/2) and human telomerase reverse transcriptase (tHERT) [7, 8].

Two distinct isoforms of sphingosine kinase (SK1 and SK2) catalyse the ATP-dependent phosphorylation of sphingosine (Sph) to produce S1P. These biochemically well-characterised enzymes are regulated in a spatial and temporal manner by post-translational modification and interaction with specific proteins and lipids (recently reviewed [9, 10]). SKs are part of a wider network of enzymes that inter-convert many sphingolipids in response to environmental change and stimuli [11]. In general, the cellular effects of S1P (proliferation, migration, differentiation, survival) are largely opposed to those of ceramide (apoptosis, senescence, growth arrest *etc*.) and the concept of the ‘sphingolipid rheostat’ was proposed, whereby the inter-conversion of ceramide, *via* sphingosine, to intracellular S1P controls cellular fate [12, 13]. A more nuanced model incorporates both the receptor-mediated and intracellular effects of S1P [14, 15]. Moreover, ceramide exists as multiple molecular species that might have differing roles and act independently of S1P in a membrane- and target-specific manner [16], including supporting proliferation [17]. Nonetheless, the therapeutic potential of SK inhibitors (to raise apoptotic ceramide and reduce S1P formation) and S1P receptor antagonists has been intensively pursued, particularly within the context of cancer (recently reviewed by Santos & Lynch [18] and Kunkel *et al*. [5], respectively). Indeed, high SK1 expression is associated with poor prognosis and disease stage in a number of cancers [19, 20]. Similarly, *in vitro* evidence, disease models and patient data support a role for SK2 in cancer [21, 22]. Thus, oncology clinical trials for two low potency SK inhibitors are on-going or completed but not yet reported. The SK2 inhibitor, ABC294640, is in trials for pancreatic cancer, solid tumours and relapsed diffuse large B-cell lymphoma. The aim of this Review is to interrogate the available SK1 crystal structures with reference to those of related lipid kinases and so provide new insight into the structural features, binding sites, mechanism and regulation of SK1.

Current structural models

Two human SK genes, *SPHK1* and *SPHK2*, give rise respectively to three SK1 splice variants (SK1a, SK1b. SK1c) and two confirmed SK2 variants (SK2a, SK2b), where the variants within each gene family differ in the length of the N-terminal sequence [14]. The first SK crystal structures were acquired with human SK1a [23]. In the absence of added ligands the protein crystallised as an asymmetric unit comprising three molecules of SK1 (PDB: 3VZB). A region of J-shaped electron density in two of the protein molecules suggested the presence of adventitious sphingoid base, with Sph providing the best fit for this feature; the third molecule was unliganded and taken to represent the protein in its apo-state. A structure (3VZC) was also obtained with crystals grown in the presence of an inhibitor, 4-((4-(4-chlorophenyl)thiazol-2-yl)amino)phenol (SKI-II, also known as SKi), targeted to the Sph binding site. The nucleotide binding site was also defined in a third structure (3VZD) following co-crystallisation with both SKI-II and ADP. Two subsequent SK1 co-crystal structures (4L02, 4V24) with potent sphingosine-competitive inhibitors have provided additional details on the interaction of ligands in the Sph binding site [24, 25]. Crystal structures for SK2 have yet to emerge and thus discussion herein is focused primarily on SK1.

SK1 overall structure and relation to DAGK_cat family proteins

SK1 has a two-domain architecture (Figure 1, Key Figure) that comprises an N-terminal domain (NTD) with a binding site for the nucleotide and a C-terminal domain (CTD) hosting the Sph binding site. The catalytic centre is located in a cleft formed at the inter-domain junction. The NTD is composed of six β-strands (β1-β5 and β17) and six α-helices (α1-α6) organised in an α/β/α sandwich. Its core is provided by a 4-stranded β-sheet, ordered as β2-β1-β3-β4, with the edge of β2 exposed on the outside surface distal to the CTD. Towards the catalytic cleft the sheet is extended by a fifth strand (β5); the C-terminal β17 strand, inserted between β5 and β4, then completes a twisted 6-stranded sheet and serves to zip the two domains together. The CTD contains 11 β-strands (β6-β16) that are organised as a two-layer β-sandwich. Three extended loops between strands β8-β9, β10-β11 and β11-β12 pack across one face to generate the Sph binding site. The sequences are designated herein 'lipid binding loop 1-3' (LBL-1 to LBL-3) respectively. LBL-1 folds with two reverse-paired helices (α7-α8) such that the inter-helix connection is orientated into the catalytic cleft. The second loop, LBL-2, which is shorter and lacks secondary structure, also interfaces with the NTD at the catalytic cleft. LBL-3 folds without making direct contact with the NTD as an additional helix (α9), running antiparallel along α8. The lipid binding site is located between the helix bundle (α7-α9) and its interface with the CTD β-sandwich. The reverse face of the β-sandwich is occupied by a single regulatory loop ('R-loop') extension between strands-β9/β10 and hosts phosphorylation sites in both SK1 and SK2 [26, 27].

Phylogramatically, SK1 and SK2 are grouped with mammalian diacylglycerol (DAG) kinase enzymes (DGKs) [28], other eukaryotic lipid kinases [29, 30] and prokaryotic enzymes of the bacterial DgkB class [31] into the **DAGK_cat family** (see Glossary). The mammalian DGKs are multi-domain containing proteins, but as yet no crystal structures are available for the catalytic domain of these enzymes or for other eukaryotic lipid kinases to facilitate comparative structure-function analysis with SK1. By contrast, nine crystal structures have become available for prokaryotic DAGK_cat relatives. The first of these were obtained for the YegS protein from *Escherichia coli* (2BON, 2JGR) [32] and its orthologue from *Salmonella typhimurium* (2P1R) [33]. DAG is not a substrate for YegS, and *in vitro* studies suggest that it may catalyse phosphorylation of phosphatidyl glycerol [32]. The first *bona fide* DGK to be structurally defined was the DgkB protein from *Staphylococcus aureus* [34]; structures obtained with and without bound ADP (2QV7, 2QVL) provided initial insights regarding organisation of the nucleotide binding site in DAGK_cat proteins. Three crystal structures for a putative DGK from *Bacillus anthracis* subsequently emerged (3S40, 3T5P, 4WRR) and one structure for a putative DGK from *Enterococcus faecalis* (4WER) [http://www.rcsb.org]. AMP is defined in the nucleotide binding site of the latter, but none of these structures are complexed with lipid substrates. All of the proteins exhibit a similar NTD fold and CTD core β-sandwich, with the two domains connected by a pair of long antiparallel strands that characteristically cross over one another at the inter-domain junction. These twisted inter-domain strands in SK1 correspond to β5+β6 in the outward (NTD-to-CTD) leg and β16+β17 in the return leg. In many DAGK_cat proteins an aspartic acid at the cross-over point contributes to a regulatory metal ion binding site [32-34]. This is absent in SK1, but, based on sequence analysis (Figure S1), might potentially be retained in SK2. Collectively the prokaryotic DAGK_cat structures exhibit strong conservation in the key structural motifs that bind ATP, but differ from SK1 in the structure of the CTD extended loops.

Substrate binding sites

The nucleotide binding site in SK1 (Figure 1) is highly homologous with the corresponding site in the prokaroytic DAGK_cat proteins; key interaction motifs are defined on the SK1 sequence presented in the supplementary material (Figure S1). The adenine is inserted into a groove between the β1-α1 and β2-α2 loops, making contacts with residues 22-NPR-24 (motif-1) and 54-TERR-57 (motif-2). Motif-3 (79-SGDGLMHE-86), a DAGK_cat signature sequence encompassing the β3-α3 loop [34], provides key contacts for the α-phosphate of the nucleotide and is often referred to as the 'P-loop'. The β-phosphate is engaged by motif-4 (111-GSGNAL-116), another DAGK_cat signature sequence. Frequently in the form of GTXND in the wider family, this motif is referred to as the 'T-loop' [34]. The catalytic Mg^{2+} ion, coordinated to the phosphates, is bound by another conserved element of DAGK_cat proteins, a DGE sequence (motif-5), through the carboxylate of Glu343 and backbone carbonyl of Asp341. The β-phosphate is also engaged by Arg185 and Arg191 from LBL-1, although the position of Arg191 is such that it might be reconfigured for binding the ATP γ-phosphate and incipient S1P product arising from catalytic turnover.

Consistent with their action on distinct substrates, the DAGK_cat proteins that have been structurally characterised to date differ significantly in the structure of their lipid binding regions, especially LBL-1 and LBL-2 (Figure S2). In the case of SK1 Sph is accommodated within a curved tube, the 'J-channel', and makes extensive surface contact with the protein, involving hydrophobic residues in the three lipid binding loops and across one face of the CTD β-sandwich core. Key residues in the binding site are largely conserved between SK1 and SK2. Differences occur at four sites, with two of these, Ile174/Met272 (Val304/Leu517 in SK2), located in the throat of the J-channel and a third, Phe288 (Cys533 in SK2), at its toe. The fourth distinguishing residue, Ala339 (Thr584 in SK2), is linked through a networked water to the Sph head group, which is highly organised through additional hydrogen bonds to Asp178/Ser168 (Figure 1). The Sph-1-OH is positioned in loose contact with P-loop Asp81, which simultaneously caps the T-loop with two hydrogen bonds at the N-terminus of helix-α5. The Sph-3-OH engages Asp178 on LBL-1 as a key anchor point (Figure 1). Co-crystal structures have been obtained with three inhibitors that all exploit J-channel occupancy (Figure S3). Two of these, Amgen-1V2 and PF-543 [24, 25], possess Sph-mimetic head groups and target Asp178 with a hydroxymethyl group in place of the Sph-3-OH. In the absence of a suitable hydroxylated ligand, as in the SKI-II-bound and apo SK1 crystal structures, the Sph-3-OH site is occupied by a surrogate water molecule, suggesting that the lipid head group interaction region involving Asp178 is highly preorganised for substrate binding in SK1.

Catalytic mechanism

At some point during catalytic turnover the phosphoacceptor hydroxyl of Sph must undergo deprotonation. P-loop residue Asp81, which is proximal to the hydroxyl in the Sph-bound crystal structure (Figure 1), has been assigned as the general base responsible for this [23]. A surprising feature, however, is the involvement of Asp81 as a doubly hydrogen bonded cap for helix-α5, which could potentially reduce its ability to function as a base. Nevertheless an available hydrogen bond site on the Asp81 carboxylate remains, and access to this site is evinced in the Sph-bound SK1 crystal structure. Asp81 is therefore implicated in the catalytic mechanism (Figure 2).

Collectively, the SK1 crystal structures reveal considerable plasticity in the β-phosphate binding T-loop, a feature that is also evident in the available prokaryotic DAGK_cat crystal structures, where it is associated with conformational switching in the capping mode of the Asp81-cognate residue. Thus, the *B. anthracis* DGK structures reveal, in one case (3S40), a doubly-capped state for the aspartate and, in two other cases (3T5P, 4WRR), a singly-capped state in which only one of the aspartate oxygens engages the T-loop whilst the second is lifted towards the site that would be occupied by the Sph-1-OH in SK1. Movement in the T-loop, dependent on nucleotide occupancy, may therefore play an important role in the mechanism, and Asp81 might possibly switch to a singly-capped T-loop mode with bound ATP, allowing optimisation of both presentation and basicity at the point of catalytic turnover. It is also conceivable that plasticity in the T-loop allows the key H-donor centres for the β-phosphate to track separation of ADP from the γ-phosphate during the reaction pathway from substrates to products. This is suggested by remarkable differences in T-loop backbone NH trajectory that distinguish the ADP-bound and nucleotide-free SK1 crystal structures.

Lipid substrate access

In general the mechanisms whereby lipid kinases locate and act on their substrates are poorly understood. Phosphorylation may occur with the lipid still anchored in a membrane in some instances [35]. However, for SK1 the complete enclosure of Sph within the CTD suggests a full lipid extraction-encapsulation action. Only a narrow entry to the J-channel exists, where it opens to the ATP binding site, and access through this point would require Sph to tunnel tail first past a guard of polar residues. A more reasonable mode of substrate entry would involve opening and closure of helices-α7/8 (LBL-1), which form a flap over the Sph binding site. The likelihood of such LBL-1 movement is suggested by the other DAGK_cat crystal structures, such as the *Enterococcus* DGK structure (4WER), where the α7-cognate region is disordered but a helix corresponding to α8 is well defined. In this case the latter helix is flipped outwards to expose both its own inner hydrophobic surface and that of the β-sandwich core (Figure 3). The helix is trapped in this open state by crystal lattice packing unique to this particular structure, but its observed position highlights the plausibility of an open-close movement in the α7/8 'lipid lid' helices. Conceivably, the catalytic action of SKs may thus function by transient opening of LBL-1 and presentation of head group-interacting residues to facilitate substrate recognition at the membrane interface, with subsequent extraction accompanied by closure of LBL-1 to encapsulate the lipid substrate.

Oligomerisation of SK1

Inspection of the available prokaryotic DAGK_cat crystal structures reveals a common pattern of dimeric assembly through NTD-NTD engagement (Figure 3). The only exception to this pattern is the aforementioned *Enterococcus* DGK crystal structure (4WER), where interlocking of the CTD LBL-1 dictates the solid state assembly. Some diversity is seen in the NTD-NTD dimerisation interfacial sequences, molecular interactions and subunit orientation, but in all cases the dimer assembly features some degree of annealing along the exposed β2 strands of the protomers. This is augmented by additional interactions involving flanking helices-α1/α2 and their connecting loops. Similar inspection of the SK1 structures reveals that in each case all of the constituent protein molecules are paired through an NTD-NTD interface with C_2-symmetry (Figure 3), suggesting that the enzyme may adopt a dimeric quaternary structure. Although oligomerisation has yet to be reported in intact non-*transfected in vivo* systems, the capacity of SK1 to dimerise is consistent with the results of immunoprecipitation experiments with expressed differentially tagged SK1 constructs in cells [36, 37]. Interface-contributory residues (identified in Figure S1) are not fully conserved between SK1 and SK2. Thus, the NTD-NTD contact for SK2 will differ from that in the SK1, if indeed SK2 dimerises through such an interface.

The β2-α2 loop (54-TERR-57), which contributes to the ATP binding site in SK1, is directly involved in cross-subunit interactions at the putative dimer interface through the side chains of Glu55/Arg56. However, comparison of the SK1 crystal structures reveals some degree of plasticity in this loop. Thus, one ('loop-out') conformation has the backbone folded towards the dimerisation interface cleft. A second ('loop-in') conformation has the backbone folded slightly into the ATP binding site. Conformational adjustment may therefore potentially influence nucleotide binding. Intriguingly an asymmetric mixed loop-out/loop-in dimer state is observed in the 3VZB crystal structure for a pairing between Sph-complexed and apo-SK1 protein molecules. Moreover, in the apo-SK1 molecule, the LBL-1 inter-helix residues exhibit some positional movement (up to 6Å) compared to SK1 molecules with ligand occupancy (Sph or inhibitor) in the CTD. This is accompanied by establishment of an inter-domain hydrogen bond between Arg57 on the β2-α2 loop and the backbone of Leu344 immediately adjacent to the DGE-motif. These observations might suggest a model where the β2-α2 loop conformation may be influenced both by the presence or absence of ligand in the lipid binding site and by a cross-subunit relay *via* the dimerisation interface within an oligomeric assembly [37, 38].

Regulatory control

Subcellular localisation of SK1 and SK2 critically underpins their biochemical roles (reviewed elsewhere [39-43]) and dictates transformation of normal cells into cancer cells [44]. In unstimulated cells SK1 is a predominantly cytosolic enzyme, but stimulation with a range of agonists can elicit both upregulation of SK1 catalytic activity [45-55] and translocation to the plasma membrane [26, 44, 56-59]. One such stimulatory pathway, that has provided a model for understanding translocation of SK1 to the plasma membrane (PM), is the response to phorbol myristate acetate (PMA) [53, 57]. This leads ultimately to phosphorylation of SK1 on Ser225, which regulates PM-targeting and enhanced SK1 activity [26]. The phosphorylation is mediated by extracellular signal-regulated kinase (ERK1/2) and is reversed by the action of protein phosphatase 2 (PP2A) [60]. Interactions with both phosphatidylserine (PS) [61, 62] and phosphatidic acid (PA) [63] have also been implicated in the activation/localisation of SK1 at the PM and endoplasmic reticulum (ER)/Golgi-apparatus. Indeed, it has been proposed that engagement of PS could involve specific recognition of the lipid head group at a site exposed in the protein upon phosphorylation of Ser225 [62]. Thr54 and Asn89 have tentatively been implicated as contributory residues to a PS-binding site, as both were shown to be important for SK1 binding to PS-derived vesicles and (in cell culture) also to the PM [62, 64].

Ser225 occupies a prominently solvent-exposed location in the R-loop, packed on the reverse side of the CTD core β-sandwich to the lipid binding site. The tip of the R-loop (231-QGP-234) packs against NTD helices-α3/4 (94-RPDW-97) and is maintained in this position by insertion of R-loop Asp235 into a pocket on the β-sandwich surface lined by His156/Arg162/His355 (Figure 4). Ser225 appears ideally poised to displace Asp235 from this pocket upon phosphorylation, and this would in turn displace the R-loop from its NTD engagement, potentially eliciting structural transition in helices-α3/4. Clues as to the possible structural impact on helices-α3/4 lie in the crystal structures of the *Staphylococcus* DgkB, which contains a helix-α3 sequence (76-NGIAEKPNR-84) homologous to that of SK1 (89-NGLMERPDW-97) but lacks the R-loop. The glutamate in this sequence engages basic residues in the CTD, whereas in SK1 it is folded back along the α3-axis to pin down the side chains of Arg61/Arg65 from the adjacent helix-α2. In principle, R-loop displacement could allow conformational relaxation in the SK1-ERPD sequence, and a direct mapping onto the cognate DgkB-EKPN motif would release Arg61/Arg65, opening a potential binding site adjacent to Asn89 (one of the residues previously implicated in PS binding). Alternatively, as the SK1 crystal structures show that Asn89 contributes a cross-domain double H-bond contact, the importance of Asn89 may lie not in direct contact with PS, but in the maintenance of appropriate NTD-CTD spacing to facilitate the postulated conformational switching of Glu93.

Thr54 adopts two distinct rotameric states in the SK1 crystal structures. In one state the hydroxyl is orientated towards the ATP binding site, as an adenine contact point, and in the second it is reversed to cap helix-α2. This conformational switching is allied to plasticity in the β2-α2 loop that affects the presentation of proximal residues defining the surface of the putative dimerisation interface cleft (His59/Glu55/Arg56) as well as Arg57 on the β2-α2 loop itself. Thus, Thr54 may play a key role in orchestrating β2-α2 loop structure to facilitate PS binding, potentially at the proposed dimerisation interface cleft. Definitive clarification of the involvement of Thr54/Asn89 in PS binding requires further structural investigation, but reconfiguration of the R-loop upon phosphorylation of Ser225 may influence the conformation of the Thr54-containing β2-α2 loop by controlling the engagement of α3-Glu93 with α2-Arg61/Arg65 as discussed above. Moreover, a strong cluster of arginines in/near to the putative dimerisation cleft (residues-16/24/56/57/61/65) could be consistent with this region of the protein acting as a contact surface for anionic phospholipids.

Although maintenance of residence at the PM requires interaction with lipids, active translocation of SK1 may be influenced by other factors, with preliminary work suggesting that calmodulin binding might be important for membrane targeting [56, 65]. Further investigation refined this understanding and identified **Calcium- and Integrin-Binding Protein (CIB1)** as the active, calcium-sensing partner that mediates translocation of SK1 [66]. The CIB1 binding site was localised to the sequence now defined as helix-α8 from the crystal structures (Figure 4), within which combined F197A/L198Q substitution was shown to ablate CIB1 binding and SK1 translocation. However, the same exposed LBL-1 hydrophobic surface has recently been implicated in direct curvature-sensitive binding of SK1 to negatively charged membranes [67]. Significantly, the exposed LBL-1 surface of both protomers is aligned along the same edge of the putative SK1 dimer. Moreover, an electrostatic potential surface map of the dimer reveals a region of high positive charge density over a concave surface separating the two LBL-1 sites (Figure 5). Docking of this surface to a convex negatively charged membrane interface might reasonably allow simultaneous embedding of both LBL-1 sites into the membrane to facilitate substrate extraction by the gating mechanism proposed in Figure 3. The postulated dimerisation of SK1 may therefore have direct bearing on curvature-sensitive membrane recruitment of the enzyme, which has been shown to be important in endocytosis [67].

The C-terminal sequence of SK1 also plays an important regulatory role, and truncation after residue 363 renders SK1a constitutively active and insensitive to stimulation by PMA [68]. This 21-residue C-terminal deletion also enhances localisation at PS-containing lipid raft microdomains without requirement for phosphorylation of Ser225. Extension by four additional residues (364-367) restores the lower basal activity levels of wild-type SK1a, but, remarkably, in a manner that is independent of residue identity. In the available crystal structures Gly364 is located immediately adjacent to the exposed C-terminus of the short helix-α5, at the opposite end to the T-loop and catalytic centre. These crystal structures were acquired with proteins truncated after Gly364, but it is clear that the peptide backbone over residues 364-367 would be well-positioned to act as a C-terminal cap for helix-α5 (Figure 6). Moreover, given the plasticity of the T-loop and its relevance to the catalytic mechanism, any leverage exerted on helix-α5 by such a cap might plausibly be relayed into the catalytic centre to modulate activity. Enhanced membrane targeting of the C-terminally truncated SK1a protein might suggest that displacement of the C-terminal sequence also unmasks the postulated anionic phospholipid binding site or frees access to the membrane binding surface of the enzyme, and, therefore, that the structural transition arising from R-loop phosphorylation might serve to modulate the interaction of the C-terminal sequence with the core catalytic domain. Sequestration of the SK1 C-terminal sequence by partner proteins might thus conceivably unmask the membrane-interacting determinants of SK1 to facilitate membrane recruitment without phosphorylation of Ser225. This could perhaps explain a finding that G_q-coupled M_3 muscarinic receptor signalling induces translocation of SK1 to the PM in a manner that is independent of Ser225 phosphorylation and changes in $[Ca^{2+}]_i$ [69]. No SK1-interacting protein partner was identified in that study, but some protein associations with the SK1 C-terminus have been established (see Figure 6). Interestingly, the position of Gly364 is such that the C-terminal sequence would project sideways and clear of the membrane surface from an SK1 dimer docked, as proposed above, through the interfacial LBL-1 motifs and positively charged groove. Protein binding to the SK1 C-terminus may, then, be feasible for such a dimer whilst actively engaged at a membrane interface.

Whilst a structural basis for regulatory control of SK1 activity and targeting has yet to be firmly established, interaction with anionic phospholipids appears to be important, and we propose that the membrane curvature-sensing property of SK1 may be related to a dimeric architecture. Membrane recruitment is clearly influenced by the phosphorylation status of the R-loop, but the evidence above suggests that the C-terminal sequence also critically affects membrane binding and catalytic activity. SK1 crystal structures with the intact C-terminus are currently not available, but an important possibility that should be considered is whether structural transition induced by phosphorylation modulates interaction of the C-terminus with the core catalytic domain to disclose the membrane-binding determinants of SK1.

Concluding remarks

In this Review we have provided an explanation of the molecular and structural organisation of SK1 as it relates to catalysis, regulatory control and the role of the enzyme in cell biology. Several new structure-function hypotheses are presented that raise key questions and provide direction for future investigation (see Outstanding Questions). An understanding of the dynamic changes in SK1 structure, which underpin its biological action in health and disease, will provide a basis for multiple approaches to target this enzyme with small molecule modulators that include both allosteric [37] and orthosteric-directed compounds.

Glossary

Calcium- and integrin-binding protein (CIB1): a ubiquitous 191-residue protein comprising globular N-terminal and C-terminal domains, each composed of two EF-hands separated by flexible linker. The two C-terminal EF-hands bind Ca^{2+} ions with affinities just above basal Ca^{2+} concentration levels. Calcium binding elicits structural transition that exposes a membrane-targeting N-terminal myristoyl group and as well a groove for partner protein interaction, the latter by unfolding of a C-terminal helix.

DAGK_cat family (Pfam 00781): a protein family that encompasses 10 mammalian diacylglycerol kinases (DGKs) together with other eukaryotic lipid kinases [ceramide kinase (CerK), a multi-substrate lipid kinase (MULK) and SKs]. Bacterial DGKs fall into two distinct classes: a group of soluble DGK proteins, denoted DgkB, that are expressed by Gram-positive organisms and belong to the DAGK_cat family; and an unrelated group of integral membrane proteins, DgkA (Pfam 01219), expressed in Gram-negative organisms.

Figure 1 caption (full-width figure) (REVIEW KEY FIGURE)

Figure 1, Key Figure. Tertiary structure and substrate binding site detail for SK1. Centre: Sph•SK1 co-crystal structure (3VZB chain A) with Sph (blue surface) encapsulated in the CTD; Mg•ADP (green sphere/pink surface) is shown superimposed from a separate SK1 co-crystal (3VZD chain C) [23]. Labelled secondary structure features correspond to the sequence mapping (Figure S1); key motifs and loops are coloured coded (see Ribbon Key). The crystal structure was acquired with a protein construct encompassing residues 9-364 of hSK1a; this construct exhibited comparable catalytic activity to the full-length enzyme of 384 residues (which failed to crystallise satisfactorily). The regulatory R-loop is fully ordered for this chain but exhibits some disorder in other chains and crystal structures, particularly in its C-terminal half including the ERK1/2 phosphorylation site (Ser225, circled). None of the available SK1 structures encompass the C-terminal 20-residue sequence that facilitates binding of PP2A (for dephosphorylation of Ser225) and mediates additional regulatory control [60, 68]. Top left and right: Binding site detail and residue interaction map for Sph (yellow stick) showing the curved fit of the lipid tail to the J-channel and highly organised polar interaction network surrounding the head group. SK2 differs (Figure S1) in binding site residues corresponding to I174, M272 and F288 (red surface) and A339. A structural water (W1), conserved in all SK1 crystal structures, and D178 engage the Sph-3-OH. The Sph-1-OH binds in two states, loosely (3.4 Å contacts) to L268 and P-loop residue D81 (catalytic base). Bottom right and left: Nucleotide binding site detail and residue interaction map showing the α- and β-phosphates engaged respectively by P-loop and T-loop.

Figure 2 caption (side-captioned figure)

Figure 2. Catalytic mechanism and protein plasticity at the catalytic centre. A mechanistic formulation for substrate phosphorylation (panel A) involves polarisation of the phosphoacceptor hydroxyl through H-bonded contact to D81 in the enzyme-substrate complex; the ensuing nucleophilic attack on the ATP γ-phosphate might then proceed with concomitant full deprotonation of the substrate hydroxyl by D81 as the putative catalytic base [23]. R185 and R191 both hydrogen bond to the nucleotide's β-phosphate in the Mg•ADP co-crystal structure (Figure 1), but with suboptimal hydrogen bond trajectory due to proximal

congestion of the juxtaposed guanidinium moieties. This suggests that R191 may preferentially bind the γ-phosphate in complex with ATP and thence to the incipient S1P phosphate during catalytic turnover. R185/R191 and residues of the T-loop exhibit significant conformational mobility across the available SK1 crystal structures. T-loop plasticity (panel B) alters backbone NH trajectory and may allow the T-loop to track separation of ADP from the γ-phosphate during the reaction course. In the wider DAGK_cat family crystal structures plasticity encompasses conformational switching of the D81-cognate residue between single and double H-bond capping of the T-loop, as illustrated for the *B. anthracis* DGK (panel C). Binding of ATP in SK1 may thus induce T-loop movement in SK1 to tighten the Sph-1-OH/D81 H-bond, potentially with D81 in a singly-capped state.

Figure 3 caption (side-captioned figure)

Figure 3. Lipid substrate entry and quaternary structure hypotheses. The available prokaroyotic DAGK_cat family structures reveal a general pattern wherein LBL-1 (cyan ribbon) is characterised by helical secondary structure elements connected to the core β-sandwich by flexible linkers (often disordered). In the *Enterococcus* DGK structure (top), the sequence corresponding to α7 in SK1 is disordered whilst the α8-cognate helix is flipped open, exposing the hydrophobic interior to accommodate the same helix (cyan mesh) from an adjacent protein molecule in the crystal lattice. This suggests that the DAGK_cat LBL-1 loop is conformationally mobile and provides a plausible mechanism for Sph entry in SK1 (centre). Analogous movement (black arrows) in helices-α7/α8 of SK1 may provide a gating mechanism for entry and exit of Sph and S1P (blue and red arrows respectively). With the exception of the *Enterococcus* DGK crystal structure, all of the other prokaryotic DAGK_cat crystal structures reveal a common pattern of dimeric assembly through NTD-NTD engagement, illustrated for the *Staphylococcus* DgkB structure (bottom). An analogous C_2-symmetric dimer assembly is observed in all five of the currently available SK1 crystal structures, which exhibit different crystallographic space groups, and may represent a *bona fide* biological oligomer. Here the putative SK1 dimer (centre) is viewed along its C_2-symmetry axis; interfacial residues are marked (red font) on the sequence in Figure S1. Some variance in subunit relative rotation is seen across the DAGK_cat dimers; the *Staphylococcus* DgkB structure (bottom) is presented with the left hand subunit aligned to the left hand SK1 protomer directly above.

Figure 4 caption (full-width figure)

Figure 4. SK1 regulatory processes and allied mechanistic hypotheses. Membrane-targeting of SK1 is influenced by phosphorylation of S225 and interaction with CIB1. The structure of SK1 is shown (centre) orientated to highlight the R-loop and position of S225, colour coding as keyed in Figure 1. The R-loop tip (231-QGP-233) makes inter-domain contact with residues (93-ERPDW-97) at the junction of helices-α3/α4, with the loop conformation controlled by insertion of D235 into a base-lined pocket (H156/R162/H355), detailed in inset A. PhosphoS225 may displace D235, with reconfiguration of the loop position (black arrows) and thence reconfiguration of the 93-ERPDW-97 residues as detailed in inset B, where the superimposed ribbon (magenta) corresponds to SK1 89-NGLMERPDW-97 mapped onto the cognate motif

(76-NGIAEKPNR-84) of the *Staphylococcus* DgkB protein (2QV7). Conformational repositioning of E93 (red arrow) could influence the orientation of α2-R61/R65, thus affecting the structure proximal to N89 or/and (*via* the β2-α2 loop) T54, these residues having been implicated in targeting to PS-rich membrane domains [62, 64]. F197/L198 (cyan stick) on helix-α8 are implicated in binding to CIB1. Potentially this might involve opening of LBL-1, as postulated for substrate access in Figure 3, freeing helix-α8 to engage the CIB1 protein interaction groove, as in inset C. Binding to CIB1, by analogy to its precedented protein associations [70-72], may require unfolding of the CIB1 C-terminal helix (purple ribbon) from the protein interaction groove. Conceivably, if SK1 translocation proceeds in an LBL-1 'loop-open' state, the displaced CIB1 helix might engage SK1 in a manner similar to that illustrated with the *Enterococcus* DGK helix insertion in Figure 3.

Figure 5 caption (full-width figure)

Figure 5. SK1 membrane engagement hypothesis. (A) Dimerisation of SK1 according to the crystallographically observed state results in presentation of the two LBL-1 lipid gate loops (cyan ribbon) on the same face of the cylindrical assembly. LBL-1 has recently been implicated [67] as a site for direct curvature-sensitive binding to negatively charged membranes, with mutagenic replacement of surface-exposed hydrophobic residues (F197/L198, cyan stick, marked) ablating membrane targeting. The location of T54, another residue shown [62, 64] to be important for binding to negatively charged membranes is marked (spheres). (B) Application of a qualitative electrostatic potential surface to the SK1 dimer, viewed from the same perspective as panel A, shows a concave positively charged surface region (green box) separating the hydrophobic LBL-1 islands (cyan circles) across the dimer interface. (C) SK1 targets narrow tubular membrane invaginations of average diameter 23 nm in an experimental model of early endocytic intermediates [67]; here an approximate scale view is shown with the SK1 dimer orientated to a convex surface corresponding to the cross section of these tubular invaginations (orange ring, membrane depth not to scale). The view perspective has SK1 orientated at right angles to that in panel A and with the surface groove aligned along the tubule axis for hypothesised interaction with anionic phospholipids (circled –ve charge). Docking in this manner might reasonably allow simultaneous embedding of both LBL-1 sites into the membrane to facilitate substrate extraction by the postulated gating mechanism (black arrows).

Figure 6 caption (side-captioned figure)

Figure 6. Regulatory and targeting hypotheses for the SK1 C-terminal sequence. (A) Available SK1 crystal structures derive from protein constructs truncated at G364 (red spheres); G364 is juxtaposed to the C-terminal end of helix-α5, which also hosts the T-loop (marked) at the catalytic centre. (B) The C-terminal tail sequence of 21 residues (365-CVEPPPSWKPQQMPPPEEPL-384) is missing from available structures but is

known to host protein binding sites: residues 379-PPEE-382 bind tumour necrosis factor receptor-associated factor 2 (TRAF2), a component in the multi-protein assembly resulting from engagement of the tumour necrosis factor (TNF) receptor [73], whilst residues 368-384 have been implicated in binding protein phosphatase 2 (PP2A) [60]. Membrane binding of the SK1 putative dimer, according to the hypothesised mode of Figure 5, would position G364 such that the missing C-terminal sequence of the two protomers (dotted red lines) could extend to engage in protein associations. In the absence of bound proteins the tail sequences may potentially fold to obstruct binding to membrane interfaces, thereby conferring cytosolic distribution; C-terminal protein association may then unmask membrane interaction determinants in SK1. Alternatively, structural transition in the R-loop elicited by phosphorylation of S225 may also promote release of the C-terminal tail to facilitate membrane targeting. (C) An expansion (orientated as in panel B) suggests that the backbone of residues 364-367 may cap helix-α5. Deletion of the C-terminal sequence activates SK1 [68], probably by altering leverage on the T-loop.

References

1. Blaho, V.A. and Hla, T. (2011) Regulation of mammalian physiology, development, and disease by the sphingosine 1-phosphate and lysophosphatidic acid receptors. *Chem. Rev.* 111, 6299-6320.
2. Spiegel, S. and Milstien, S. (2011) The outs and the ins of sphingosine-1-phosphate in immunity. *Nat. Rev. Immunol.* 11, 403-415.
3. Maceyka, M. and Spiegel, S. (2014) Sphingolipid metabolites in inflammatory disease. *Nature* 510, 58-67.
4. Pyne, S. and Pyne, N.J. (2011) Translational aspects of sphingosine 1-phosphate biology. *Trends Mol. Med.* 17, 463-472.
5. Kunkel, G.T., *et al.* (2013) Targeting the sphingosine-1-phosphate axis in cancer, inflammation and beyond. *Nat. Rev. Drug. Discov.* 12, 688-702.
6. Kihara, Y., *et al.* (2014) Lysophospholipid receptor nomenclature review: IUPHAR Review 8. *Br. J. Pharmacol.* 171, 3575-3594.
7. Hait, N.C., *et al.* (2009) Regulation of histone acetylation in the nucleus by sphingosine-1-phosphate. *Science* 325, 1254-1257.
8. Panneer Selvam, S., *et al.* (2015) Binding of the sphingolipid S1P to hTERT stabilizes telomerase at the nuclear periphery by allosterically mimicking protein phosphorylation. *Sci. Signal.* 8, ra58.
9. Chan, H. and Pitson, S.M. (2013) Post-translational regulation of sphingosine kinases. *Biochim. Biophys. Acta* 1831, 147-156.
10. Neubauer, H.A. and Pitson, S.M. (2013) Roles, regulation and inhibitors of sphingosine kinase 2. *FEBS J.* 280, 5317-5336.
11. Hannun, Y.A. and Obeid, L.M. (2008) Principles of bioactive lipid signalling: lessons from sphingolipids. *Nat. Rev. Mol. Cell Biol.* 9, 139-150.
12. Pyne, S., *et al.* (1996) Sphingomyelin-derived lipids differentially regulate the extracellular signal-regulated kinase 2 (ERK-2) and c-Jun N-terminal kinase (JNK) signal cascades in airway smooth muscle. *Eur. J. Biochem.* 237, 819-826.
13. Cuvillier, O., *et al.* (1996) Suppression of ceramide-mediated programmed cell death by sphingosine-1-phosphate. *Nature* 381, 800-803.
14. Pyne, S., *et al.* (2009) Role of sphingosine kinases and lipid phosphate phosphatases in regulating spatial sphingosine 1-phosphate signalling in health and disease. *Cell. Signal.* 21, 14-21.
15. Newton, J., *et al.* (2015) Revisiting the sphingolipid rheostat: Evolving concepts in cancer therapy. *Exp. Cell. Res.* 333, 195-200.
16. Hannun, Y.A. and Obeid, L.M. (2011) Many ceramides. *J. Biol. Chem.* 286, 27855-27862.

17. Saddoughi, S.A. and Ogretmen, B. (2013) Diverse functions of ceramide in cancer cell death and proliferation. *Adv. Cancer Res.* 117, 37-58.
18. Santos, W.L. and Lynch, K.R. (2015) Drugging Sphingosine Kinases. *ACS Chem. Biol.* 10, 225-233.
19. Pyne, N.J. and Pyne, S. (2010) Sphingosine 1-phosphate and cancer. *Nat. Rev. Cancer* 10, 489-503.
20. Long, J.S.*, et al.* (2010) Sphingosine kinase 1 induces tolerance to human epidermal growth factor receptor 2 and prevents formation of a migratory phenotype in response to sphingosine 1-phosphate in estrogen receptor-positive breast cancer cells. *Mol. Cell. Biol.* 30, 3827-3841.
21. Gao, P. and Smith, C.D. (2011) Ablation of sphingosine kinase-2 inhibits tumor cell proliferation and migration. *Mol. Cancer Res.* 9, 1509-1519.
22. Wallington-Beddoe, C.T.*, et al.* (2014) Sphingosine kinase 2 promotes acute lymphoblastic leukemia by enhancing MYC expression. *Cancer Res.* 74, 2803-2815.
23. Wang, Z.*, et al.* (2013) Molecular basis of sphingosine kinase 1 substrate recognition and catalysis. *Structure* 21, 798-809.
24. Gustin, D.J.*, et al.* (2013) Structure guided design of a series of sphingosine kinase (SphK) inhibitors. *Bioorg. Med. Chem. Lett.* 23, 4608-4616.
25. Wang, J.*, et al.* (2014) Crystal Structure of Sphingosine Kinase 1 with PF-543. *ACS Med. Chem. Lett.* 5, 1329-1333.
26. Pitson, S.M.*, et al.* (2003) Activation of sphingosine kinase 1 by ERK1/2-mediated phosphorylation. *EMBO J.* 22, 5491-5500.
27. Hait, N.C.*, et al.* (2007) Sphingosine kinase type 2 activation by ERK-mediated phosphorylation. *J. Biol. Chem.* 282, 12058-12065.
28. Topham, M.K. and Epand, R.M. (2009) Mammalian diacylglycerol kinases: molecular interactions and biological functions of selected isoforms. *Biochim. Biophys. Acta* 1790, 416-424.
29. Waggoner, D.W.*, et al.* (2004) MuLK, a eukaryotic multi-substrate lipid kinase. *J. Biol. Chem.* 279, 38228-38235.
30. Spiegel, S. and Milstien, S. (2007) Functions of the multifaceted family of sphingosine kinases and some close relatives. *J. Biol. Chem.* 282, 2125-2129.
31. Zhang, Y.M. and Rock, C.O. (2008) Membrane lipid homeostasis in bacteria. *Nat. Rev. Microbiol.* 6, 222-233.
32. Bakali, H.M.*, et al.* (2007) Crystal structure of YegS, a homologue to the mammalian diacylglycerol kinases, reveals a novel regulatory metal binding site. *J. Biol. Chem.* 282, 19644-19652.
33. Nichols, C.E.*, et al.* (2007) Characterization of Salmonella typhimurium YegS, a putative lipid kinase homologous to eukaryotic sphingosine and diacylglycerol kinases. *Proteins* 68, 13-25.
34. Miller, D.J.*, et al.* (2008) Analysis of the Staphylococcus aureus DgkB structure reveals a common catalytic mechanism for the soluble diacylglycerol kinases. *Structure* 16, 1036-1046.
35. Emptage, R.P.*, et al.* (2014) Structural basis of lipid binding for the membrane-embedded tetraacyldisaccharide-1-phosphate 4'-kinase LpxK. *J. Biol. Chem.* 289, 24059-24068.
36. Liu, Z.*, et al.* (2013) Synthesis of (S)-FTY720 vinylphosphonate analogues and evaluation of their potential as sphingosine kinase 1 inhibitors and activators. *Bioorg. Med. Chem.* 21, 2503-2510.
37. Lim, K.G.*, et al.* (2011) FTY720 analogues as sphingosine kinase 1 inhibitors: enzyme inhibition kinetics, allosterism, proteasomal degradation, and actin rearrangement in MCF-7 breast cancer cells. *J. Biol. Chem.* 286, 18633-18640.
38. Kihara, A.*, et al.* (2006) Mouse sphingosine kinase isoforms SPHK1a and SPHK1b differ in enzymatic traits including stability, localization, modification, and oligomerization. *J. Biol. Chem.* 281, 4532-4539.
39. Wattenberg, B.W.*, et al.* (2006) The sphingosine and diacylglycerol kinase superfamily of signaling kinases: localization as a key to signaling function. *J. Lipid Res.* 47, 1128-1139.
40. Wattenberg, B.W. (2010) Role of sphingosine kinase localization in sphingolipid signaling. *World J. Biol. Chem.* 1, 362-368.
41. Siow, D. and Wattenberg, B. (2011) The compartmentalization and translocation of the sphingosine kinases: mechanisms and functions in cell signaling and sphingolipid metabolism. *Crit. Rev. Biochem. Mol. Biol.* 46, 365-375.
42. Siow, D.L.*, et al.* (2011) Sphingosine kinase localization in the control of sphingolipid metabolism. *Adv. Enzyme Regul.* 51, 229-244.

43. Pitson, S.M. (2011) Regulation of sphingosine kinase and sphingolipid signaling. *Trends Biochem. Sci.* 36, 97-107.
44. Pitson, S.M., *et al.* (2005) Phosphorylation-dependent translocation of sphingosine kinase to the plasma membrane drives its oncogenic signalling. *J. Exp. Med.* 201, 49-54.
45. Olivera, A. and Spiegel, S. (1993) Sphingosine-1-phosphate as second messenger in cell proliferation induced by PDGF and FCS mitogens. *Nature* 365, 557-560.
46. Rius, R.A., *et al.* (1997) Activation of sphingosine kinase in pheochromocytoma PC12 neuronal cells in response to trophic factors. *FEBS Lett.* 417, 173-176.
47. Xia, P., *et al.* (1998) Tumor necrosis factor-alpha induces adhesion molecule expression through the sphingosine kinase pathway. *Proc. Natl. Acad. Sci. U. S. A.* 95, 14196-14201.
48. Meyer zu Heringdorf, D., *et al.* (1999) Role of sphingosine kinase in Ca(2+) signalling by epidermal growth factor receptor. *FEBS Lett.* 461, 217-222.
49. Alemany, R., *et al.* (1999) Formyl peptide receptor signaling in HL-60 cells through sphingosine kinase. *J. Biol. Chem.* 274, 3994-3999.
50. Young, K.W., *et al.* (1999) Lysophosphatidic acid-mediated Ca2+ mobilization in human SH-SY5Y neuroblastoma cells is independent of phosphoinositide signalling, but dependent on sphingosine kinase activation. *Biochem. J.* 343 Pt 1, 45-52.
51. Meyer zu Heringdorf, D., *et al.* (2001) Stimulation of intracellular sphingosine-1-phosphate production by G-protein-coupled sphingosine-1-phosphate receptors. *Eur. J. Pharmacol.* 414, 145-154.
52. Blaukat, A. and Dikic, I. (2001) Activation of sphingosine kinase by the bradykinin B2 receptor and its implication in regulation of the ERK/MAP kinase pathway. *Biol. Chem.* 382, 135-139.
53. Shu, X., *et al.* (2002) Sphingosine kinase mediates vascular endothelial growth factor-induced activation of ras and mitogen-activated protein kinases. *Mol. Cell. Biol.* 22, 7758-7768.
54. MacKinnon, A.C., *et al.* (2002) Sphingosine kinase: a point of convergence in the action of diverse neutrophil priming agents. *J. Immunol.* 169, 6394-6400.
55. Mastrandrea, L.D., *et al.* (2005) Sphingosine kinase activity and sphingosine-1 phosphate production in rat pancreatic islets and INS-1 cells: response to cytokines. *Diabetes* 54, 1429-1436.
56. Young, K.W., *et al.* (2003) Ca2+/calmodulin-dependent translocation of sphingosine kinase: role in plasma membrane relocation but not activation. *Cell Calcium* 33, 119-128.
57. Johnson, K.R., *et al.* (2002) PKC-dependent activation of sphingosine kinase 1 and translocation to the plasma membrane. Extracellular release of sphingosine-1-phosphate induced by phorbol 12-myristate 13-acetate (PMA). *J. Biol. Chem.* 277, 35257-35262.
58. Rosenfeldt, H.M., *et al.* (2001) EDG-1 links the PDGF receptor to Src and focal adhesion kinase activation leading to lamellipodia formation and cell migration. *FASEB J.* 15, 2649-2659.
59. Melendez, A.J. and Ibrahim, F.B. (2004) Antisense knockdown of sphingosine kinase 1 in human macrophages inhibits C5a receptor-dependent signal transduction, Ca2+ signals, enzyme release, cytokine production, and chemotaxis. *J. Immunol.* 173, 1596-1603.
60. Barr, R.K., *et al.* (2008) Deactivation of sphingosine kinase 1 by protein phosphatase 2A. *J. Biol. Chem.* 283, 34994-35002.
61. Olivera, A., *et al.* (1996) Effect of acidic phospholipids on sphingosine kinase. *J. Cell. Biochem.* 60, 529-537.
62. Stahelin, R.V., *et al.* (2005) The mechanism of membrane targeting of human sphingosine kinase 1. *J. Biol. Chem.* 280, 43030-43038.
63. Delon, C., *et al.* (2004) Sphingosine kinase 1 is an intracellular effector of phosphatidic acid. *J. Biol. Chem.* 279, 44763-44774.
64. Hengst, J.A., *et al.* (2009) Sphingosine kinase 1 localized to the plasma membrane lipid raft microdomain overcomes serum deprivation induced growth inhibition. *Arch. Biochem. Biophys.* 492, 62-73.
65. Sutherland, C.M., *et al.* (2006) The calmodulin-binding site of sphingosine kinase and its role in agonist-dependent translocation of sphingosine kinase 1 to the plasma membrane. *J. Biol. Chem.* 281, 11693-11701.
66. Jarman, K.E., *et al.* (2010) Translocation of sphingosine kinase 1 to the plasma membrane is mediated by calcium- and integrin-binding protein 1. *J. Biol. Chem.* 285, 483-492.

67. Shen, H., *et al.* (2014) Coupling between endocytosis and sphingosine kinase 1 recruitment. *Nat. Cell Biol.* 16, 652-662.
68. Hengst, J.A., *et al.* (2010) Enhancement of sphingosine kinase 1 catalytic activity by deletion of 21 amino acids from the COOH-terminus. *Arch. Biochem. Biophys.* 494, 23-31.
69. ter Braak, M., *et al.* (2009) Galpha(q)-mediated plasma membrane translocation of sphingosine kinase-1 and cross-activation of S1P receptors. *Biochim. Biophys. Acta* 1791, 357-370.
70. Yamniuk, A.P., *et al.* (2006) The interaction between calcium- and integrin-binding protein 1 and the alphaIIb integrin cytoplasmic domain involves a novel C-terminal displacement mechanism. *J. Biol. Chem.* 281, 26455-26464.
71. Huang, H., *et al.* (2011) Solution structures of Ca2+-CIB1 and Mg2+-CIB1 and their interactions with the platelet integrin αIIb cytoplasmic domain. *J. Biol. Chem.* 286, 17181-17192.
72. Freeman, T.C., Jr., *et al.* (2013) Identification of novel integrin binding partners for calcium and integrin binding protein 1 (CIB1): structural and thermodynamic basis of CIB1 promiscuity. *Biochemistry* 52, 7082-7090.
73. Xia, P., *et al.* (2002) Sphingosine kinase interacts with TRAF2 and dissects tumor necrosis factor-alpha signaling. *J. Biol. Chem.* 277, 7996-8003.

Key Figure 1

Click here to download Key Figure Key Figure_new1_COMPOSITE_CMYK.tif

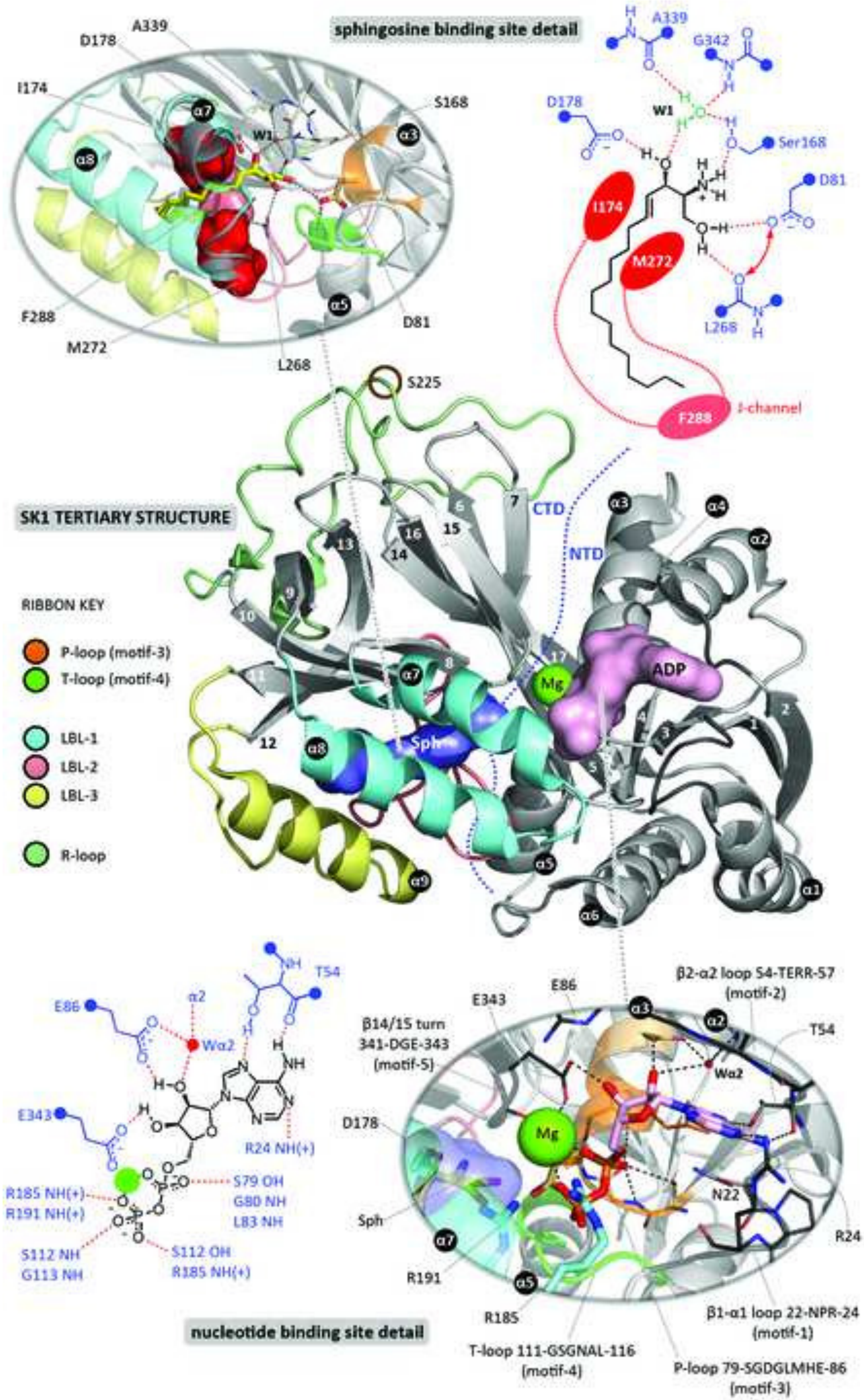

Figure 2

Click here to download Figure
Figure_new2_COMPOSITE_CMYK.tif

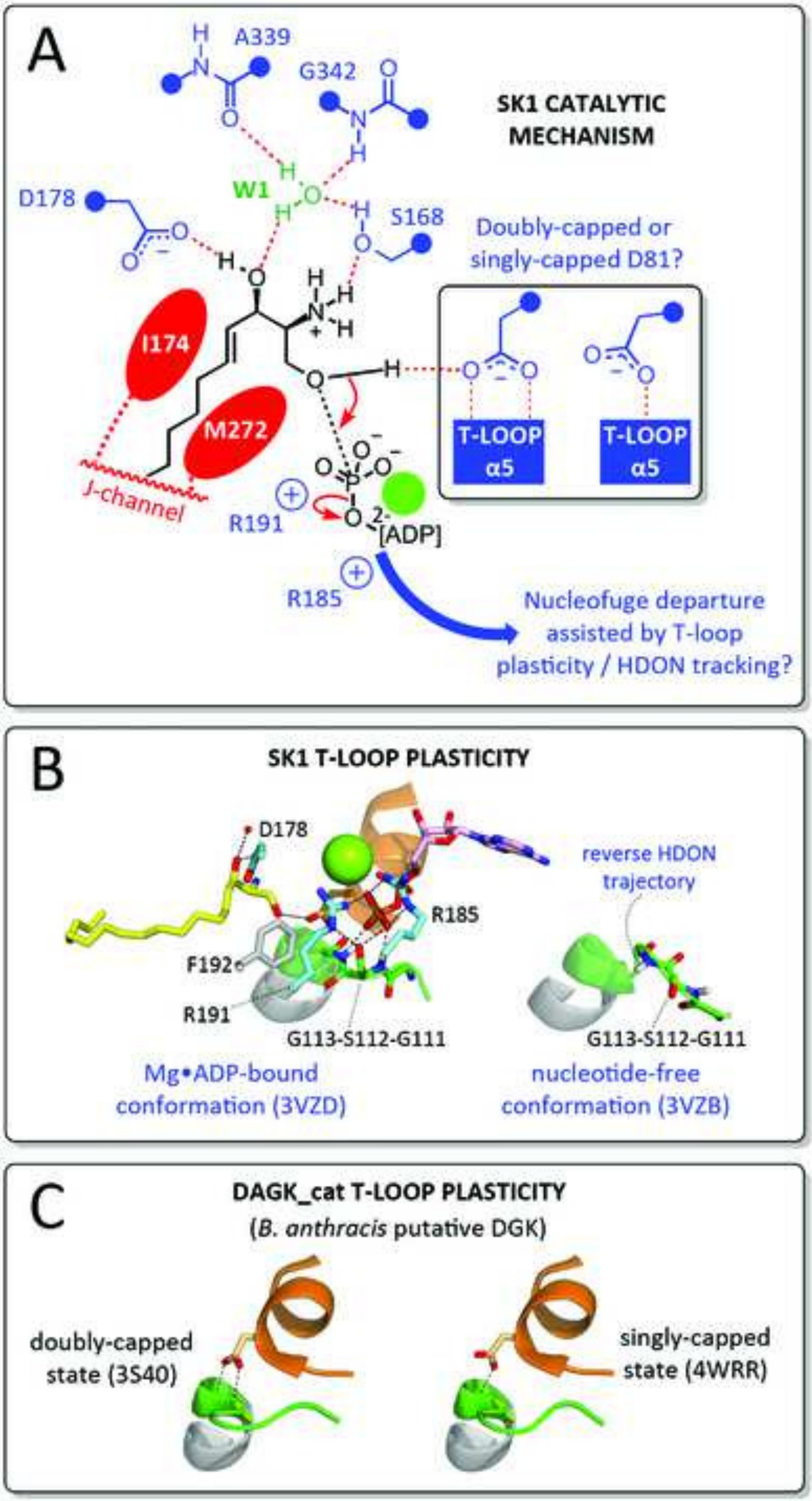

Figure 3

Click here to download Figure
Figure_new3_COMPOSITE_CMYK.tif

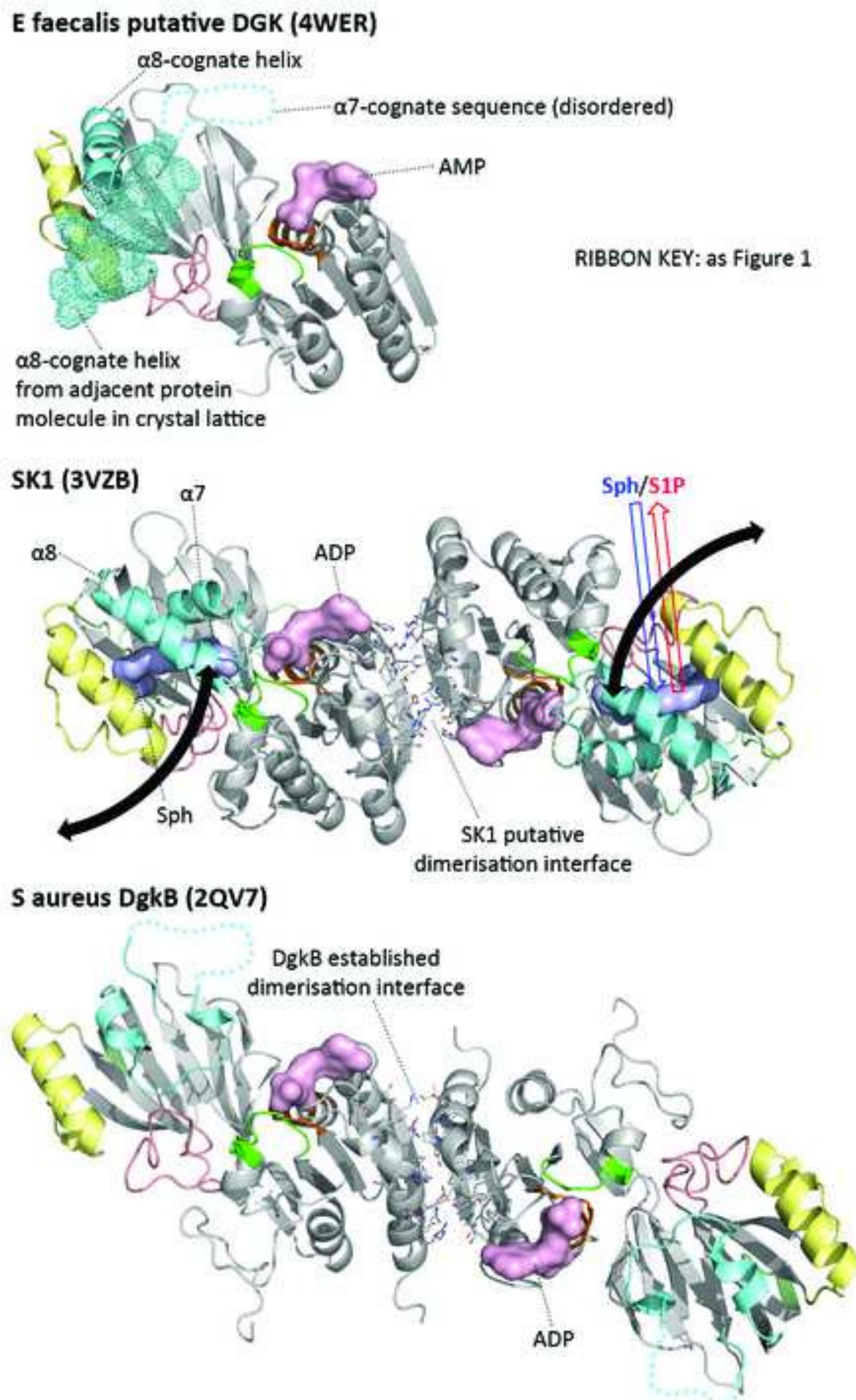

Figure 4

Click here to download Figure Figure_new4_COMPOSITE_CMYK.tif

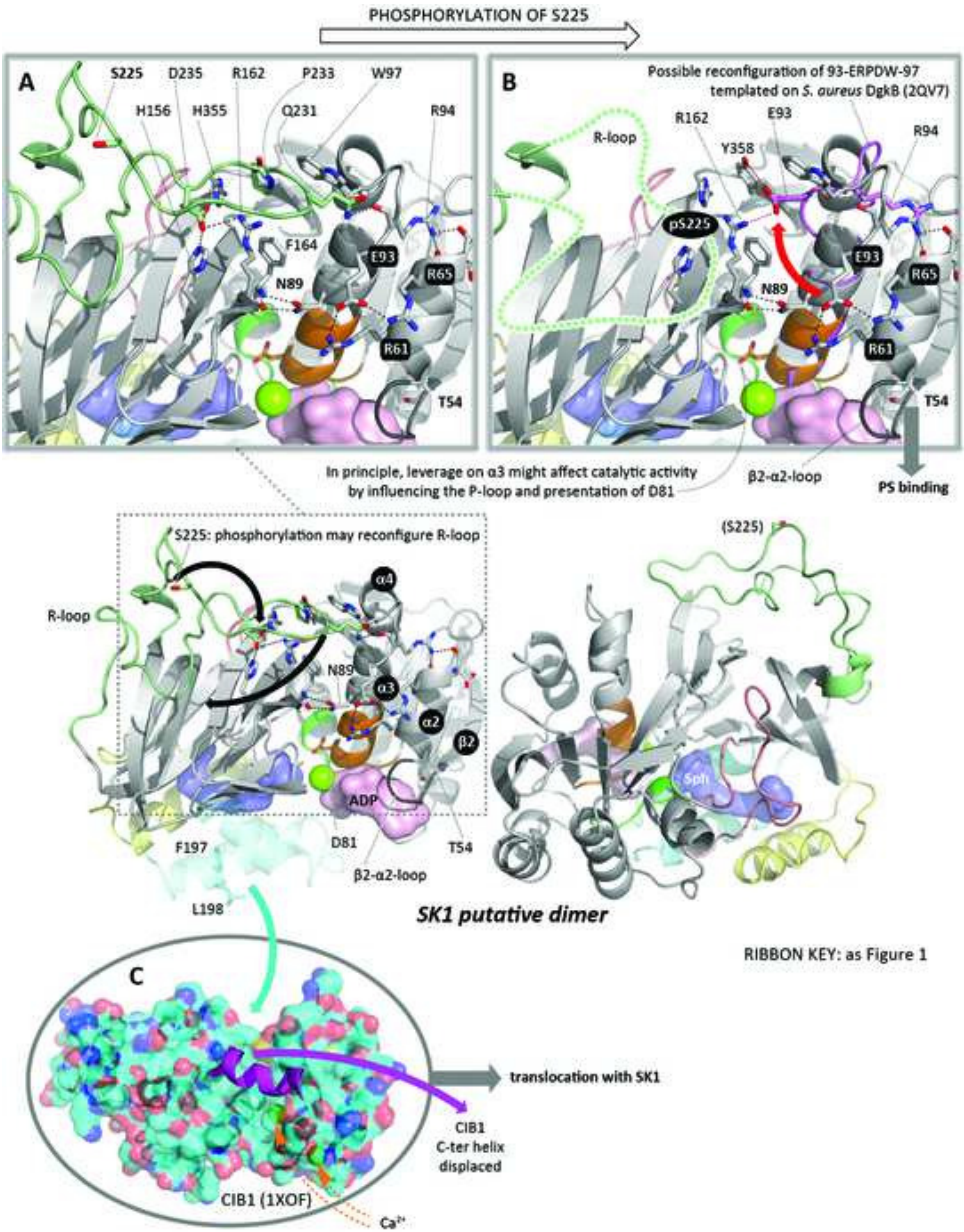

Figure 5

Click here to download Figure
Figure_new5_COMPOSITE_CMYK.tif

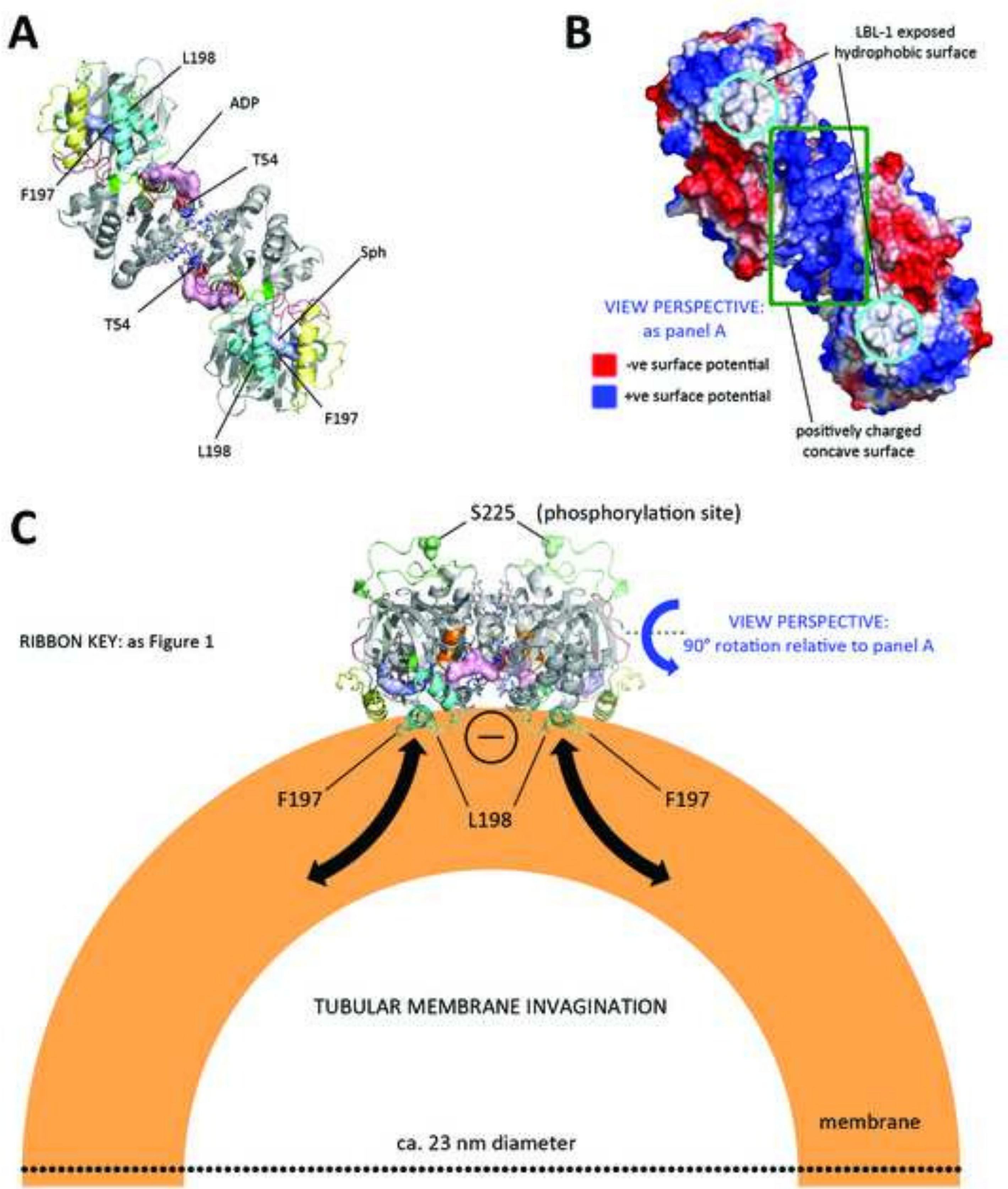

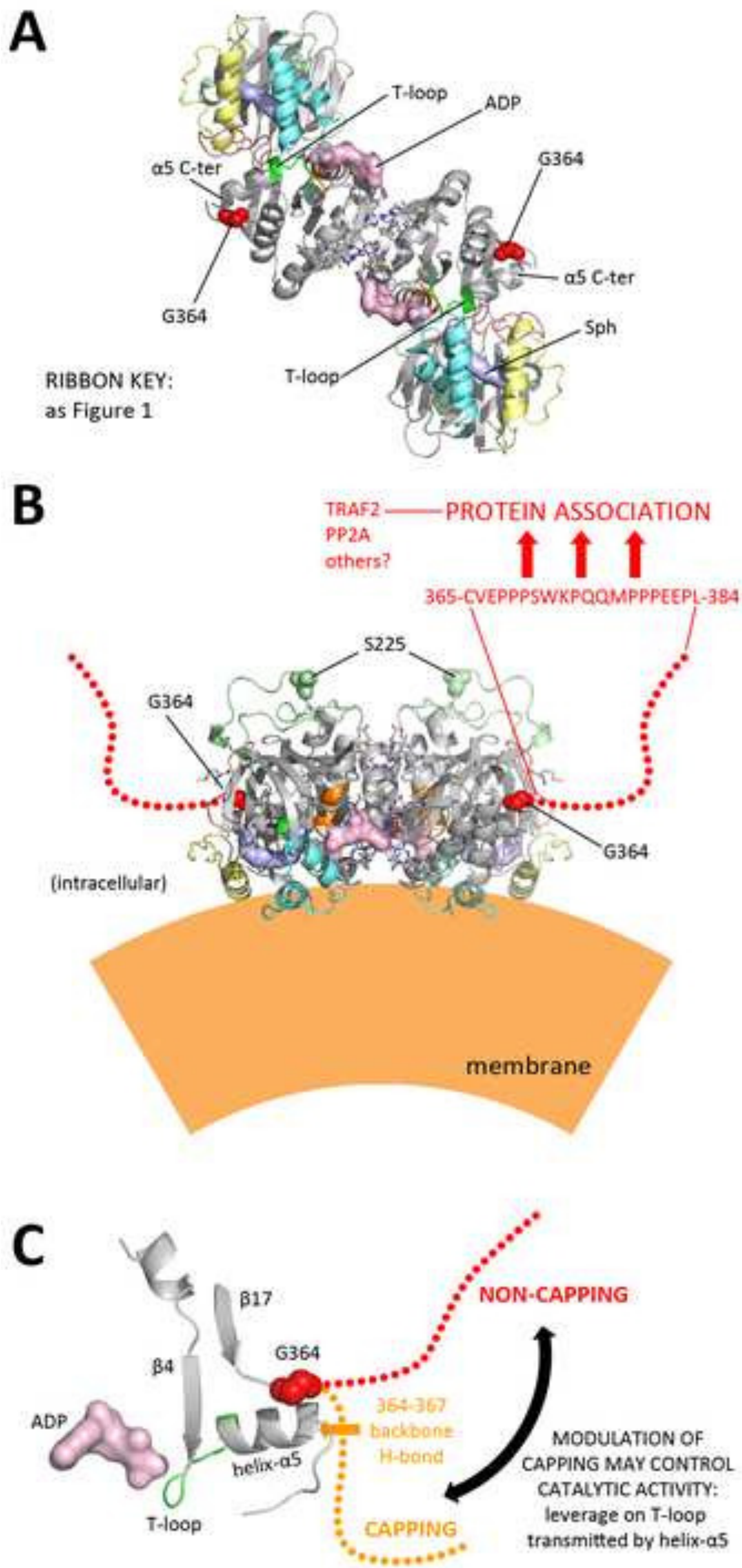
A
T-loop
ADP
α5 C-ter
G364
G364
α5 C-ter
G364
Sph
T-loop
RIBBON KEY:
as Figure 1
B
TRAF2
PP2A
others?
PROTEIN ASSOCIATION
365-CVEPPPSWKPQQMPPPEEPL-384
S225
G364
G364
(intracellular)
membrane
C
β17
NON-CAPPING
β4
G364
ADP
364-367
backbone
H-bond
helix-α5
T-loop
CAPPING
MODULATION OF
CAPPING MAY CONTROL
CATALYTIC ACTIVITY:
leverage on T-loop
transmitted by helix-α5

Supplemental Information

Sphingosine kinases: emerging structure-function insights

David R. Adams[1], Susan Pyne[2] and Nigel J Pyne[2*]

[1]Institute of Chemical Sciences, Heriot-Watt University, Edinburgh, EH14 4AS, Scotland, UK; [2]Strathclyde Institute of Pharmacy and Biomedical Sciences, University of Strathclyde, 161 Cathedral St, Glasgow, G4 0RE, Scotland, UK

*Correspondence: n.j.pyne@strath.ac.uk

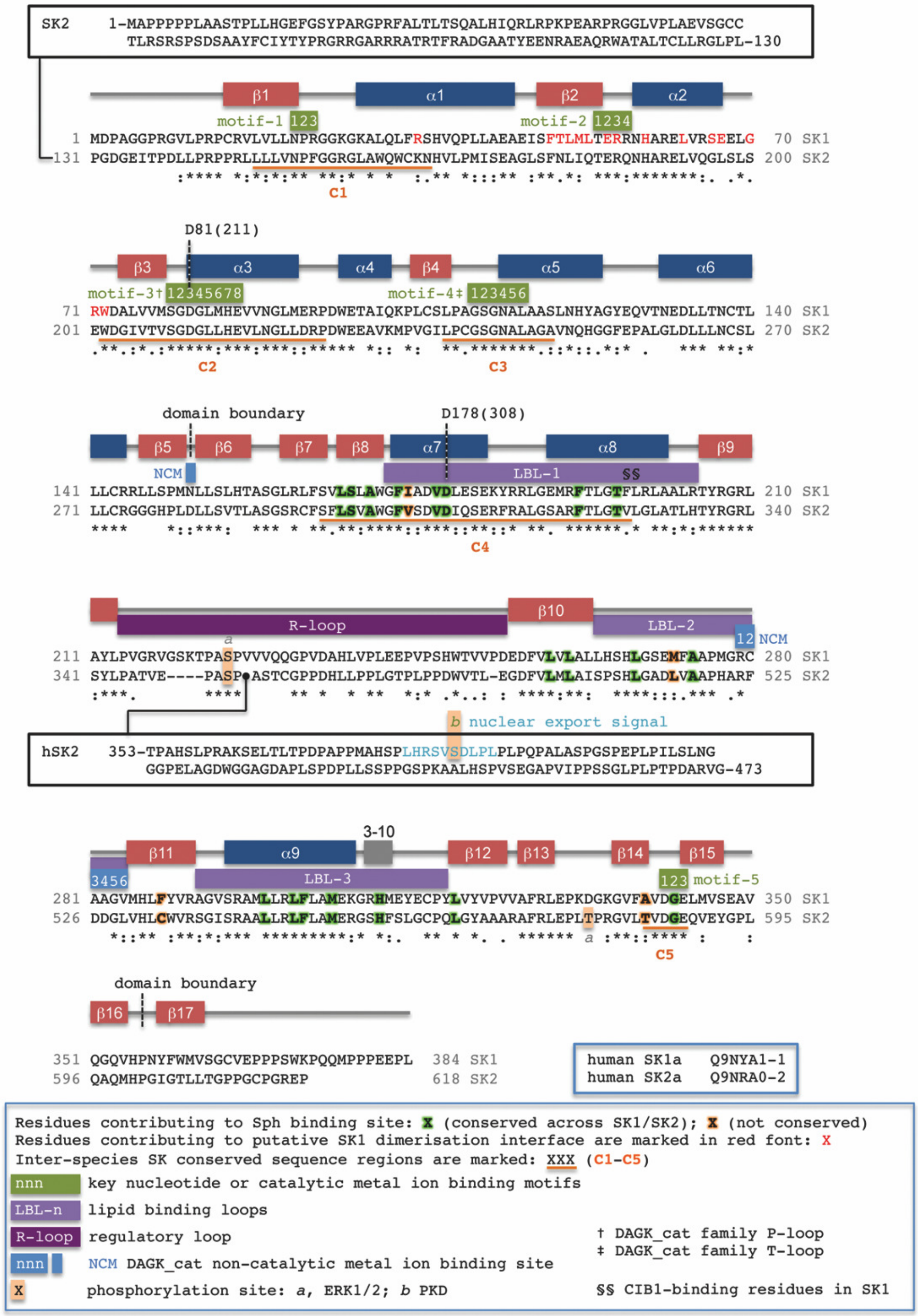

Figure S1. SK sequence alignment, secondary structure and key feature map. Multiple N-terminal splice variants have been identified from both mammalian SK genes [S1]; the alignment here uses SK1a and SK2a, UniProt entries Q9NYA1-1 and Q9NRA0-1 respectively [http://www.uniprot.org/]. Alignments with other DAGK_cat proteins have been published elsewhere [S2, S3]. Five regions (C1-C5) that are highly conserved in SK1 and SK2 across species are marked (orange underline) [S4]. Key structural features (motifs-1 to -5) that bind the nucleotide and/or catalytic metal ion are also highlighted (olive boxes, with white numbering to designate residue position). Extended loops that contribute to Sph binding (LBL-1 to LBL-3) and regulatory control (R-loop) are identified (violet boxes). Sph-interacting aspartates D81/D178 are identified (SK2 numbers in parenthesis). Structurally characterised prokaryotic DAGK_cat relatives lack the R-loop but exhibit a non-catalytic metal binding site (NCM, blue box) involving an aspartate, corresponding to Asn151 in SK1, at the centre of a twisted inter-domain strand pair. The ion is bound by an additional encircling loop, corresponding to 280-RCAAGV-285 in SK1, through backbone carbonyl coordination from residues in the P1/P6-positions and by an aspartate in the P4-position. Although the NCM-loop is retained in SK1, neither of the essential aspartates is conserved. By contrast, SK2 possesses both aspartates (Asp281/Asp527) and a loop sequence (524-RFDDGL-529) commensurate with metal-binding capacity. The role of the DAGK_cat NCM-site is not fully understood, but has been implicated in a Ca2+-activation mechanism in YegS and porcine DGKα [S2, S5].

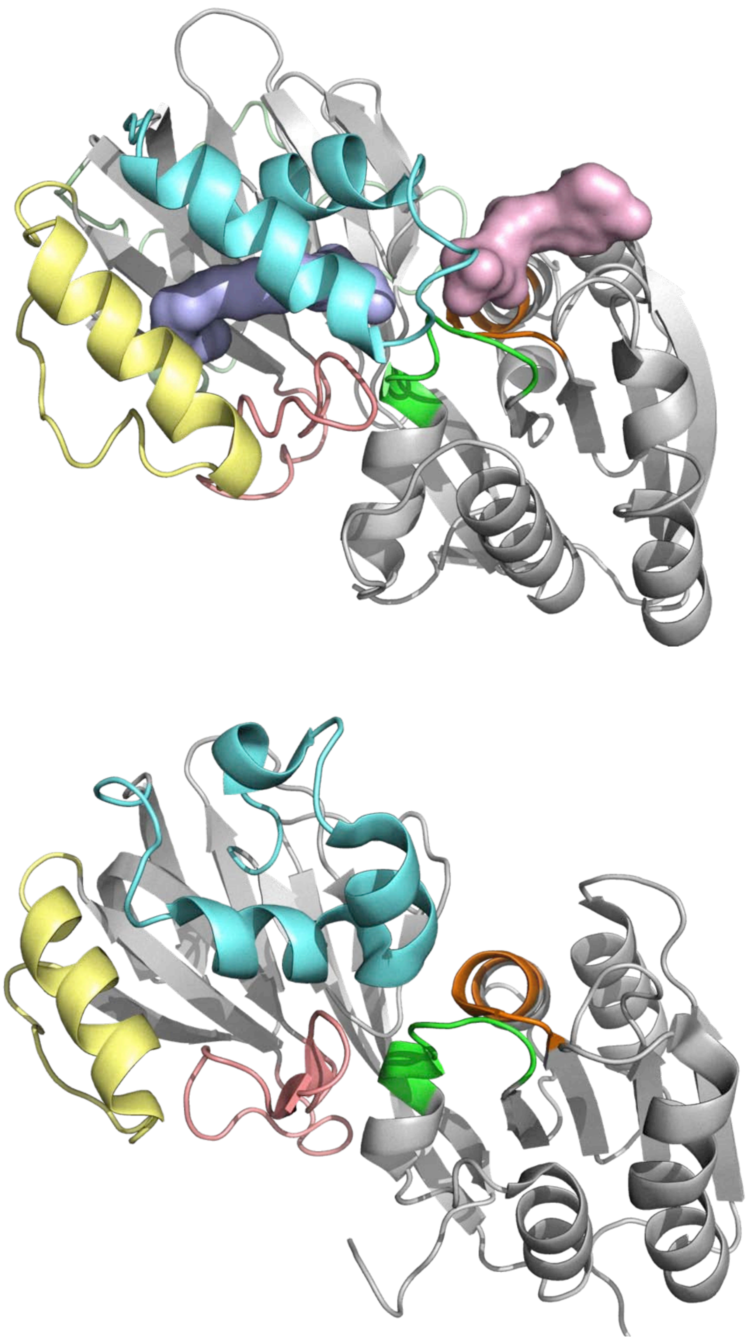

Figure S2. Comparison of tertiary structure for human SK1 and B. anthracis DGK. Top: SK1 co-crystal structure (3VZB chain A) with bound Sph (blue surface) and ADP (pink surface) superimposed from its (separate) SK1 co-crystal structure (3VZD chain C). Bottom: corresponding view of the *B. anthracis* putative DGK crystal structure (3T5P chain B) colour coded to match the SK1 structure (Ribbon key: see main text, Figure 1). Inspection of the DAGK_cat structures collectively reveals a general pattern wherein LBL-1 (cyan) is characterised by helical secondary structure elements connected by flexible linkers (disordered in several of the crystal structures) to the core β-sandwich. Thus, the *B. anthracis* DGK structures (3S40, 3T5P, 4WRR) exhibit a twin-helix organisation to LBL-1, but, as shown here (bottom), with a helix collapsed against the hydrophobic inner surface of the CTD core β-sandwich, occupying the region corresponding to the Sph binding J-channel of SK1. At present it is unclear whether the DGK might act on its lipid substrate whilst still membrane embedded or whether it might operate through an extraction-encapsulation mechanism similar to that postulated for SK1. In principle, the LBL-1 motif of the *B. anthracis* DGK might undergo conformational reorganisation to provide a more capacious lipid binding pocket in the CTD suitable for the encapsulation of a larger DAG substrate.

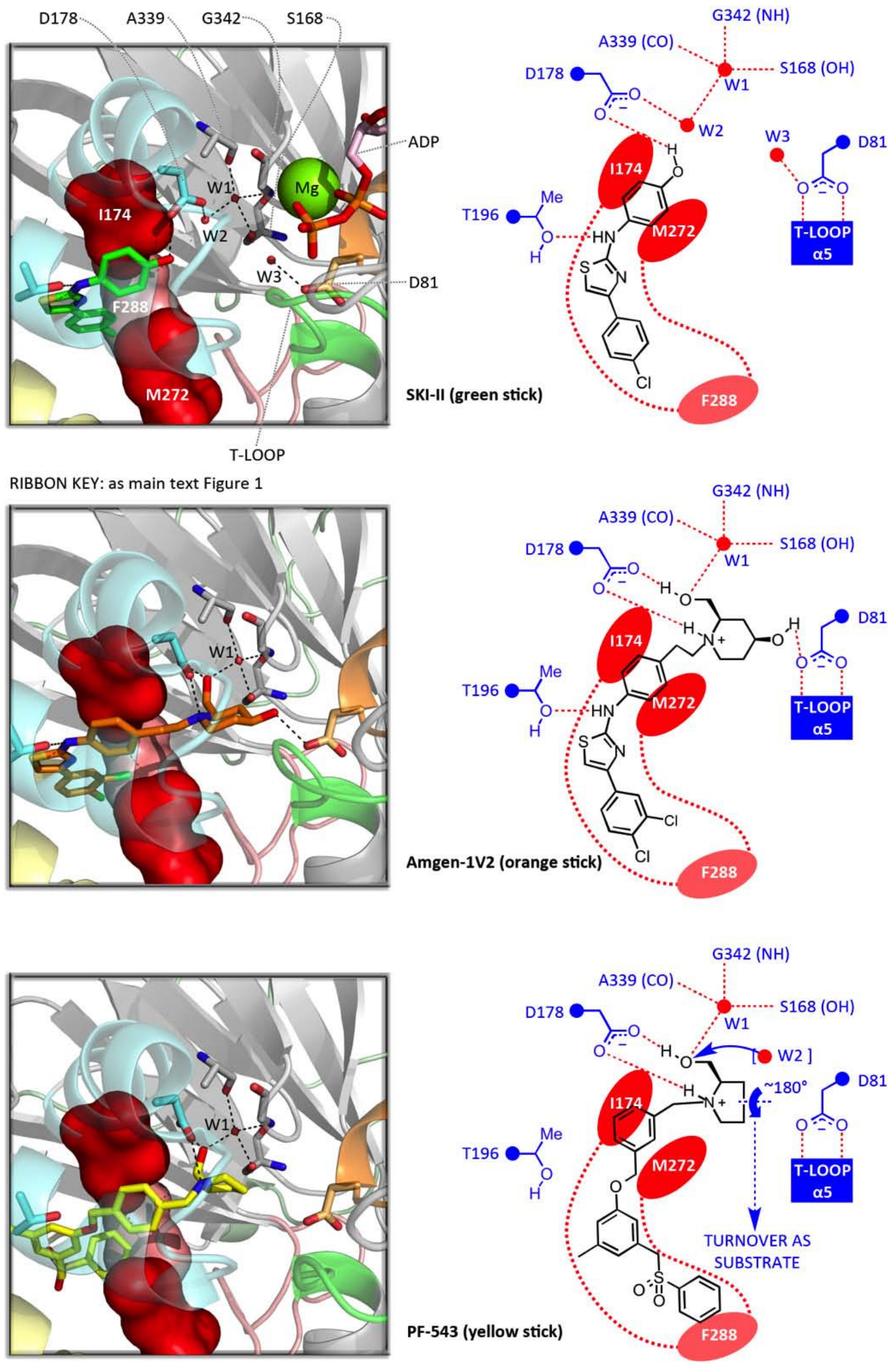

Figure S3. SK inhibitors with crystallographically-defined binding modes and residue interaction maps. Top row: SKI-II (green stick) is shown from the ternary co-crystal structure (3VZD-C) with Mg•ADP [S6]. The inhibitor binds deep in the J-channel, hydrogen bonding to α7-D178 and α8-T196. It lacks a Sph-mimetic head group and the position of the Sph-3-OH is taken by a water molecule (W2), also seen in the apo-SK1 structure (3VZB-C). W2 surrogacy provides water-bridged conservation of the connectivity between D178 and A339/G342/S168, suggesting that this network is an integral structural feature and that SK1 is highly preorganised for substrate binding. A third water (W3) approximates to the Sph-1-OH position but is more tightly hydrogen bonded to D81. The looser engagement of D81 by Sph (main text, Figure 1) suggests that the substrate is anchored in the J-channel and that some P-loop/T-loop movement may occur upon ATP binding to tighten the Sph-1-OH/D81 interaction for deprotonation. Centre row: Modification of SKI-II with a Sph-mimetic head group afforded ‘Amgen-1V2’, shown here (orange stick) from its SK1 co-crystal structure (4L02) [S7]. The inhibitor’s hydroxymethyl group occupies the Sph-3-OH position, obviating a requirement for W2 surrogacy; its 2°-hydroxyl engages D81 (close to the W3 position) whilst the piperidinium nitrogen adds a salt bridge with D178. Bottom row: PF-543 is shown (yellow stick) from its SK1 co-crystal structure (4V24) [S8]. The (hydroxymethyl)pyrrolidine binds with similar interactions to the (hydroxymethyl)piperidine of Amgen-1V2. Head group rotation, probably with concomitant W2 occupancy, would place the hydroxymethyl group close to the Sph-1-OH position, accounting for its known weak substrate character [S9].

Supplemental references

S1. Siow, D. and Wattenberg, B. (2011) The compartmentalization and translocation of the sphingosine kinases: mechanisms and functions in cell signaling and sphingolipid metabolism. Crit. Rev. Biochem. Mol. Biol. 46, 365-375.

S2. Bakali, H.M., et al. (2007) Crystal structure of YegS, a homologue to the mammalian diacylglycerol kinases, reveals a novel regulatory metal binding site. J. Biol. Chem. 282, 19644-19652.

S3. Miller, D.J., et al. (2008) Analysis of the Staphylococcus aureus DgkB structure reveals a common catalytic mechanism for the soluble diacylglycerol kinases. Structure 16, 1036-1046.

S4. Wattenberg, B.W., et al. (2006) The sphingosine and diacylglycerol kinase superfamily of signaling kinases: localization as a key to signaling function. J. Lipid Res. 47, 1128-1139.

S5. Abe, T., et al. (2003) Site-directed mutagenesis of the active site of diacylglycerol kinase alpha: calcium and phosphatidylserine stimulate enzyme activity via distinct mechanisms. Biochem. J. 375, 673-680.

S6. Wang, Z., et al. (2013) Molecular basis of sphingosine kinase 1 substrate recognition and catalysis. Structure 21, 798-809.

S7. Gustin, D.J., et al. (2013) Structure guided design of a series of sphingosine kinase (SphK) inhibitors. Bioorg. Med. Chem. Lett. 23, 4608-4616.

S8. Wang, J., et al. (2014) Crystal Structure of Sphingosine Kinase 1 with PF-543. ACS Med. Chem. Lett. 5, 1329-1333.

S9. Schnute, M.E., et al. (2012) Modulation of cellular S1P levels with a novel, potent and specific inhibitor of sphingosine kinase-1. Biochem. J. 444, 79-88.